Time and Frequency Response of Avalanche Photodiodes with Arbitrary Structure

Gokalp Kahraman, *Student Member, IEEE*, Bahaa E. A. Saleh, *Fellow, IEEE*, Winslow L. Sargeant, *Student Member, IEEE*, and Malvin C. Teich, *Fellow, IEEE*

***Abstract*—A method is developed for solving the coupled transport equations that describe the electron and hole currents in a double-carrier multiplication (DCM) avalanche photodiode (APD) of arbitrary structure. This solution permits us to determine the time and frequency response of the device. The injection can be localized to one or both ends of the multiplication region, or distributed throughout an extended region where multiplication can occur concurrently. The results are applied to conventional APD's with position-dependent carrier ionization rates (e.g., a separate-absorption-grading-multiplication APD) as well as to superlattice multiquantum-well (MQW) structures where the ionizations are localized to bandgap transition regions. The analysis may also be used to determine the dark current and include the carrier trapping at the heterojunction interfaces. Our results indicate that previous time-dependent theories only account for the tail of the time reponse under high-gain conditions and are inaccurate for high-speed devices.**

I. Introduction

With the recent advances in high-data-rate fiber-optic communication systems, there has been substantial interest in avalanche photodiodes (APD's). New structures have been introduced to enhance the gain and speed of these devices, and reduce their noise. Numerous theories have been developed for the analysis of APD's. However, since these new APD's involve inherently position-dependent carrier ionization rates and velocities, the analysis is rather difficult.

The mean photocurrent response of a conventional APD (CAPD) was initially calculated by Emmons [1], [2] by solving the carrier transport equations assuming that the ionization rates and velocities were independent of position within the multiplication region. Single-carrier injection at one end of the multiplication region was assumed. Lee *et al.* [3] and Chang [4] separately investigated the frequency variation of the multiplication process in DCM-CAPD's when the period of the sinusoidally modulated detected light is much larger than the carrier transit times. Naqvi [5] used Lee *et al.*'s assumptions to determine a frequency-dependent multiplication factor due to injection of carriers at any position and combined it with McIntyre's noise analysis [6] to derive the mean-square noise current as a function of the modulation frequency. Riad and Hayes [7] determined the frequency response of a back-illuminated InGaAsP APD with an exponentially decaying photoabsorption profile and position-dependent ionization rate, assuming single-carrier multiplication (SCM). Riad and Riad [8] used numerical methods to determine the frequency response in the double-carrier multiplication (CAPD) case.

Many researchers used Naqvi's theory in the optimization and design of low-noise large gain-bandwidth product separate/absorption/grading/multiplication (SAGM) APD's [9]–[18]. Jhee *et al.* [9] found Emmon's theory inconsistent with their calculated values of the effective transit time because their SAGM devices had nonuniform ionization rates. Campbell *et al.* [10] found Naqvi's theory in closer agreement even though they assumed equal electron and hole velocities. They [11] also proposed a method for improved frequency response by increasing (decreasing) the carrier concentration (width) of the multiplication region.

Shiba *et al.* [12] studied the frequency response of an InGaAs avalanche photodiode by solving transport equations with position-dependent ionization rates. However, in their calculations they neglected the effect of the grading and absorption regions on the device performance. They also did not indicate how they obtained their solutions. Recently. Campbell *et al.* [13] studied the multiplication noise of SAGM APD's with improved frequency response and suggested that a sufficiently general conventional theory is needed to include all the aspects of their devices (such as position dependence of ionization rates, and distributed injection). Osaka and Mikawa [14] rejected the assumption that no multiplication would occur in the absorption region under the electric fields necessary to extend the depletion region deeply into the absorption region and studied the effect of ionization within the absorption layer of an SAGM-APD on the device gain and excess noise factor under steady-state conditions.

Matsuo *et al.* [19] investigated the time dynamics of

Manuscript received November 14, 1990; revised June 18, 1991. This work was supported by the National Science Foundation. The review of this paper was arranged by Associate Editor G. Craford.

G. Kahraman, B. E. A. Saleh, and W. L. Sargeant are with the Department of Electrical and Computer Engineering, University of Wisconsin, Madison, WI 53706-1691.

M. C. Teich is with the Center for Telecommunications Research, Department of Electrical Engineering, Columbia University, New York, NY 10027.

IEEE Log Number 9105333.

SCM in superlattice devices where the ionization rates were localized at a finite number of stages, and obtained the response of the CAPD in the limit of a large number of stages [20]. Brennan *et al.* [21], [22] used Monte Carlo calculations to find the electron and hole ionization probabilities and compared the multiquantum-well (MQW), graded barrier, and doped quantum-well GaInAs/AlInAs APD's based on their gain–bandwidth product and excess noise factor. However, they calculated the bandwidth based on a formula that neglects the avalanche buildup time and therefore becomes inaccurate for DCM devices. Fyath and O'Reilly [23] and Chakrabarti and Pal [24], [25] separately applied Naqvi's theory to superlattice APD's and studied their gain–bandwidth product.

Hakim *et al.* [26] presented a general steady-state analysis of the gain and the excess noise factor in an APD of arbitrary structure in which position-dependent ionization rates, double-carrier multiplication, and dark current were included. Hollenhorst [27] introduced a new method to obtain the steady-state gain and excess noise factor for arbitrary structures with localized injection. He obtained formulas for a staircase APD with identical stages, and for an InGaAs/InP separate-absorption-multiplication (SAM) APD where the ionization rates in the two regions were assumed to be constant but different.

In this paper we provide a method to analyze the mean gain and mean-frequency response of avalanche photodiodes with arbitrary structure. In particular, this method is very convenient to analyze SAGM APD's accounting for spatial variation of ionization rates, multiplication in the absorption region, and quantum efficiency. It provides a more accurate evaluation of the 3-dB bandwidth of high-speed SAGM and superlattice MQW APD's in which the mean gain is contained within the transient part of the impulse response. Hole accumulation can also be accounted for by modeling it with an incremental region at the heterojunction surfaces characterized by a very low hole velocity. Dark current can be easily incorporated by introducing a constant carrier-generation function. Superlattice APD's are also analyzed by letting the ionization rates become large within an incremental layer at the bandgap transition regions.

We first solve the coupled transport equations which describe the electron and hole currents for an avalanche photodiode with arbitrary structure. The injection can be localized to one or both ends of the multiplication region, or distributed throughout an extended region where multiplication can occur concurrently. Then we analyze two SAPD's and an MQW APD. Their frequency-response functions and impulse-response functions are found.

Our results indicate that Naqvi's theory [5] underestimates the 3-dB bandwidth of the mean-frequency response of a high-speed APD by neglecting the transient part of the current response assuming high gain and low-frequency modulation. Our results are in close agreement with those reported by Campbell *et al.* We confirm the arguments and findings of Osaka *et al.* regarding the exact evaluation of multiplication occurring in the absorption region. We find that the frequency response cannot be improved indefinitely by shortening the multiplication region and that tunneling is not the ultimate limit for it. Rather, it is the multiplication within the absorption region which increases the avalanche buildup time and makes the device noisier. This happens because shorter multiplication regions at the electric-field levels sufficient to extend the depletion region into the absorption layer are also large enough to permit multiplication. This often makes the device unstable because of the very-large ionization rates. On the other hand, if the multiplication in the absorption region and instability were to be avoided by lowering the applied voltage, then the quantum efficiency would become unacceptably small. Therefore, an optimum structure with sufficiently large gain and quantum efficiency should be found for which both noise is suppressed and bandwidth is improved. Such an optimization and design will be the subject of a later publication.

II. Theory

A. Basic Transport Equations

Under high reverse-biasing electric fields, the carrier transport equations in the depletion region of a p-n junction take the form [1], [10]

$$\frac{\partial J_e}{\partial x} + \frac{1}{v_e}\frac{\partial J_e}{\partial t} = \alpha(x)J_e(x, t) + \beta(x)J_h(x, t) + q\phi(x, t) \tag{1}$$

$$-\frac{\partial J_h}{\partial x} + \frac{1}{v_h}\frac{\partial J_h}{\partial t} = \alpha(x)J_e(x, t) + \beta(x)J_h(x, t) + q\phi(x, t) \tag{2}$$

where $J_e(x, t)$ and $J_h(x, t)$ are the electron and hole current densities at position $x \in [0, W]$, W being the depletion-region width. The ionization rates $\alpha(x)$ and $\beta(x)$ are functions of the electric field, and $\phi(x, t)$ is the spontaneous or photo-induced rate of generation of electron–hole pairs at x, and q is the electron charge. These partial differential equations must be solved, given the boundary condition of an injected electron current $J_e(0, t) = \delta(t)$ at $x = 0$, and/or an injected hole current $J_h(W, t) = \delta(t)$ at $x = W$. Once $J_e(x, t)$ and $J_h(x, t)$ are determined, the total current induced in the external circuit that results from charge transport within the device is

$$J(t) = \frac{1}{W}\int_{x=0}^{W} [J_e(x, t) + J_h(x, t)]\, dx. \tag{3}$$

Since we are only concerned with the stable solutions. Laplace transform techniques can be used. If $J_e(x, s)$, $J_h(x, s)$, and $\phi(x, s)$ are the Laplace transform of $J_e(x, t)$, $J_h(x, t)$, and $\phi(x, t)$, respectively, then (1) and (2) give

$$\frac{\partial}{\partial x}\boldsymbol{J}(x, s) = \boldsymbol{A}(x, s)\boldsymbol{J}(x, s) + \phi(x, s)\boldsymbol{I} \tag{4}$$

where

$$\boldsymbol{A}(x, s) = \begin{bmatrix} \alpha(x) - s/v_e & \beta(x) \\ -\alpha(x) & s/v_h - \beta(x) \end{bmatrix} = \begin{bmatrix} a & b \\ c & d \end{bmatrix}$$

$$\boldsymbol{J}(x, s) = \begin{bmatrix} J_e(x, s) \\ J_h(x, s) \end{bmatrix}$$

and

$$\boldsymbol{I} = q \begin{bmatrix} 1 \\ -1 \end{bmatrix}.$$

The Laplace transform of the total current then becomes

$$J(s) = \frac{1}{W} \int_{x=0}^{W} [J_e(x, s) + J_h(x, s)]\, dx. \tag{5}$$

It is difficult to solve (4) in the general case when A is a function of x, but analytical solutions exist for constant A. Our approach is to divide the depletion layer of the device into incremental layers within each of which α and β are assumed constant, so that

$$\alpha(x) = \alpha_i \qquad \beta(x) = \beta_i \qquad \phi(x, s) = \phi_i(s)$$

$$\boldsymbol{A}(x, s) = \boldsymbol{A}_i(s), \qquad \text{for } x \in [x_{i-1}, x_i], \qquad i = 1, \cdots, N$$

with $x_0 = 0$, and $x_N = W$. We solve (4) for $x \in [x_{i-1}, x_i]$ with arbitrary boundary value $\boldsymbol{J}(x_i, s)$ and obtain the overall solution by matching the solutions at the layer boundaries.

Since analytical exact solution is obtained within each incremental layer, computation is straightforward. However, our computation method can be improved if the ionization rates could be approximated by piecewise-linear functions rather than by constants. However, even a linear dependence of the matrix $\boldsymbol{A}(x)$ does not permit an analytical solution to (4). If $\boldsymbol{A}(x)$ could be decomposed into other special matrices which are suitable for analytical solution then computation time would decrease and convergence would be faster [28], [29].

B. Solution in a Single Layer

After diagonalizing the matrix $\boldsymbol{A}_i(s)$, the solution within the ith layer is

$$\boldsymbol{J}(x, s) = \boldsymbol{P}_i(x, s)\boldsymbol{J}(x_{i-1}, s) + \boldsymbol{G}_i(x, s), \qquad x \in [x_{i-1}, x_i], \qquad i = 1, \cdots, N \tag{6}$$

where

$$\boldsymbol{P}_i(x, s) = \exp\,[\boldsymbol{A}_i(x - x_{i-1})] = \begin{bmatrix} A_i(x - x_{i-1}, s) & B_i(x - x_{i-1}, s) \\ C_i(x - x_{i-1}, s) & D_i(x - x_{i-1}, s) \end{bmatrix}$$

$$\boldsymbol{G}_i(x, s) = \phi_i(s) \int_{x_{i-1}}^{x} \exp\,[\boldsymbol{A}_i(x - x')]\boldsymbol{I}\, dx' = \begin{bmatrix} G_{i1}(x, s) \\ G_{i2}(x, s) \end{bmatrix}$$

and

$$A_i(x, s) = \Lambda_1(x, s) + a\Lambda_2(x, s) \qquad B_i(x, s) = b\Lambda_2(x, s)$$

$$C_i(x, s) = c\Lambda_2(x, s) \qquad D_i(x, s) = \Lambda_1(x, s) + d\Lambda_2(x, s)$$

$$G_{i1}(x, s) = \frac{\phi_i(s)}{\lambda_2 - \lambda_1} [(\lambda_2 - a + b)\zeta_1(x) + (a - b - \lambda_1)\zeta_2(x)]$$

$$G_{i2}(x, s) = \frac{\phi_i(s)}{\lambda_2 - \lambda_1} [(-\lambda_2 - c + d)\zeta_1(x) + (c - d + \lambda_1)\zeta_2(x)]$$

with

$$\Lambda_1(x, s) = \frac{\lambda_2 \exp(\lambda_1 x) - \lambda_1 \exp(\lambda_2 x)}{\lambda_2 - \lambda_1}$$

$$\Lambda_2(x, s) = \frac{\exp(\lambda_2 x) - \exp(\lambda_1 x)}{\lambda_2 - \lambda_1}$$

$$\zeta_1(x, s) = \frac{\exp[\lambda_1(x - x_{i-1})] - 1}{\lambda_1}$$

$$\zeta_2(x, s) = \frac{\exp[\lambda_2(x - x_{i-1})] - 1}{\lambda_2}.$$

λ_1 and λ_2 are the eigenvalues of $\boldsymbol{A}_i$ and are given as

$$\lambda_{1,2} = \frac{(a + d) \pm \sqrt{(a + d)^2 - 4(ad - bc)}}{2}.$$

λ_1, λ_2, Λ_1, Λ_2, ζ_1, ζ_2, and a, b, c, d all depend on i; their indices have been suppressed for convenience.

C. Overall Solution

We now combine the solutions at the different layers and match the boundary values to obtain the overall solution. Denoting $\boldsymbol{J}_i = \boldsymbol{J}_i(x_i, s)$, $\boldsymbol{P}_i = \boldsymbol{P}_i(x_i, s)$, and $\boldsymbol{G}_i = \boldsymbol{G}_i(x_i, s)$, and using (6), we get the recursion formula for the boundary values

$$\boldsymbol{J}_i = \boldsymbol{P}_i\boldsymbol{J}_{i-1} + \boldsymbol{G}_i, \qquad i = 1, \cdots, N. \tag{7}$$

If $\boldsymbol{J}_0$ were known, $\boldsymbol{J}_i$ could be determined by applying (7) iteratively. Since $\boldsymbol{J}_0$ is not known, we relate $\boldsymbol{J}_N$ to $\boldsymbol{J}_0$ by successive application of (7) to obtain

$$\boldsymbol{J}_N = \boldsymbol{R}\boldsymbol{J}_0 + \boldsymbol{H} \tag{8}$$

where

$$\boldsymbol{R} = \prod_{j=1}^{N} \boldsymbol{P}_i = \begin{bmatrix} R_{11} & R_{12} \\ R_{21} & R_{22} \end{bmatrix}$$

$$\boldsymbol{H} = \sum_{k=1}^{N-1} \left\{ \prod_{j=k+1}^{N} \boldsymbol{P}_i \right\} \boldsymbol{G}_k + \boldsymbol{G}_N = \begin{bmatrix} H_1 \\ H_2 \end{bmatrix}.$$

Since $J_e(W, s)$ and $J_h(0, s)$ are the only two unknowns in

the vector equation (8), it can be solved, yielding

$$J_h(0, s) = \frac{J_h(W, s) - H_2 - R_{21}J_e(0, s)}{R_{22}}$$

so that the vector

$$\boldsymbol{J}_0 = \boldsymbol{J}(0, s) = \begin{bmatrix} J_e(0, s) \\ J_h(0, s) \end{bmatrix}$$

is determined.

D. Impulse Response Function

The total current density in (5) can now be expressed as a sum

$$\begin{aligned} J(s) &= \frac{1}{W}\sum_{i=1}^{N}\int_{x_{i-1}}^{x_i}[J_e(x, s) + J_h(x, s)]\,dx \\ &= \frac{1}{W}\sum_{i=1}^{N}(A_i + C_i)J_e(x_{i-1}) \\ &\quad + (B_i + D_i)J_h(x_{i-1}) + G_{i1} + G_{i2} \end{aligned} \tag{9}$$

where A_i, B_i, C_i, D_i, G_{i1}, and G_{i2} are the integrals of $A_i(x)$, $B_i(x)$, $C_i(x)$, $G_{i1}(x)$, and $G_{i2}(x)$, respectively, within the ith layer. They are given by

$$A_i = \frac{(\lambda_2 - a)\zeta_1' - (\lambda_1 - a)\zeta_2'}{\lambda_2 - \lambda_1}$$

$$B_i = b\frac{\zeta_1' - \zeta_2'}{\lambda_2 - \lambda_1}$$

$$C_i = c\frac{\zeta_2' - \zeta_1'}{\lambda_2 - \lambda_1}$$

$$D_i = \frac{(\lambda_2 - d)\zeta_1' - (\lambda_1 - d)\zeta_2'}{\lambda_2 - \lambda_1}$$

and

$$G_{i1} = \frac{\phi_i(s)}{\lambda_2 - \lambda_1}\left\{\frac{\lambda_2 - a + b}{\lambda_1}(\zeta_1' - l_i) + \frac{a - b - \lambda_1}{\lambda_2}(\zeta_2' - l_i)\right\}$$

$$G_{i2} = \frac{\phi_i(s)}{\lambda_2 - \lambda_1}\left\{\frac{-\lambda_2 - c + d}{\lambda_1}(\zeta_1' - l_i) + \frac{c - d - \lambda_1}{\lambda_2}(\zeta_2' - l_i)\right\}$$

where

$$\zeta_1' = \frac{\exp(\lambda_1 l_i) - 1}{\lambda_1}$$

and

$$\zeta_2' = \frac{\exp(\lambda_2 l_i) - 1}{\lambda_2}.$$

Equations (7) and (9) describe the total electric current in the device for any carrier ionizations rates, velocities, and generation rates.

The frequency response function of the device (i.e., the response to a harmonically modulated light intensity) is $J(j2\pi f)$. The impulse response function $J(t)$ is the inverse Laplace transform of $J(s)$ when $\phi(x, t)$ is an impulse in time, i.e., equals $g(x)\,\delta(t)$.

E. Gain

The value of $J(j2\pi f)$ at $f = 0$ (which is equal to the area under $J(t)$) is the gain. We have verified numerically that this gain is consistent with the conventional formula. In the literature superlattice devices are often described by discrete localized multiplication regions in which the distributed ionization coefficients α and β are lumped into probabilities P and Q. The foregoing analysis, however, used the general case of the continuous ionization rates. Therefore, for the sake of comparison, correspondence between α, β and P, Q is derived in the following. The general gain formula is [6], [14]

$$M = \frac{J_{e0} + J_{hw}\exp\left[-\int_0^x(\alpha(x') - \beta(x'))\,dx'\right] + q\int_0^W g(x)\exp\left[-\int_0^x(\alpha(x') - \beta(x'))\,dx'\right]dx}{J_0\left\{1 - \int_0^W \alpha(x)\exp\left[-\int_0^x(\alpha(x') - \beta(x'))\,dx'\right]dx\right\}} \tag{10}$$

where J_{e0} and J_{hw} are electron and hole injection currents, respectively, $g(x)$ is the carrier injection rate distribution, and J_0 is the total injected current

$$J_0 = J_{e0} + J_{hw} + q\int_{x=0}^{W} g(x)\,dx. \tag{11}$$

For the case of electron injection only, $J_{hw} = 0$ and $g(x) = 0$, whereupon the gain simplifies to

$$M_n = \frac{1}{1 - \int_0^W \alpha(x)\exp\left[-\int_0^x(\alpha(x') - \beta(x'))\,dx'\right]dx}. \tag{12}$$

Since $\alpha(x)$ is zero everywhere except in the ionization regions as shown in Fig. 1, the outer integral will only need be evaluated within these regions. By evaluating the

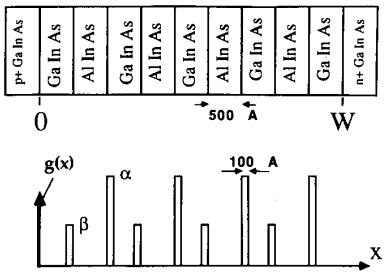

Fig. 1. The device structure and the ionization rate profiles for $Ga_{0.47}In_{0.53}As/Al_{0.48}In_{0.52}As$ simple multiquantum-well APD. There are nine 500-Å layers with 100-Å wide ionization regions at their interfaces. The electron and hole ionization rates are $\alpha = 4.57 \times 10^5$ cm^{-1} and $\beta = 5.45 \times 10^4$ cm^{-1}, within the ionization regions, and zero outside. These rates correspond to probability of ionization $P = 0.58$ for electrons and $Q = 0.056$ for holes. Single electron injection is assumed at the left-most layer so that $g(x)$ is a delta function at $x = 0$.

integral for x in the kth region, and summing for all such identical regions each with width D, we get

$$M_n = \frac{1}{1 - \sum_{k=1}^{N} e^{-kD(\alpha-\beta)}(e^{\alpha D} - 1)}.$$

Now, by defining P and Q such that

$$P = \exp\left[\int_S \alpha(x)\,dx\right] - 1 = e^{\alpha D} - 1$$

and

$$Q = \exp\left[\int_S \beta(x)\,dx\right] - 1 = e^{\beta D} - 1,$$

where S indicates that the integral is over one stage, we obtain the well-known discrete formula [5]

$$M_n = \frac{(P - Q)(1 + P)^N}{P(1 + Q)^{N+1} - Q(1 + P)^{N+1}}. \tag{13}$$

III. Applications

We have applied the foregoing equations to two different APD structures; a superlattice multiquantum-well APD and a conventional multilayer APD.

A. Superlattice or Multilayer Heterojunction APD

The first example is a $Ga_{0.4}In_{0.53}As/Al_{0.48}In_{0.52}As$ simple multiquantum-well APD in which electrons and holes ionize at abrupt bandgap transition regions [22]. The device structure and the ionization rate profile is illustrated in Fig. 1. There are nine 500-Å layers with 100-Å long ionization regions at their interfaces. The electron and hole ionization rates are $\alpha = 4.57 \times 10^5$ cm^{-1} and $\beta = 5.45 \times 10^4$ cm^{-1}, respectively, within these regions, and zero outside. These rates correspond to $P = 0.58$ and $Q = 0.056$, which are plausible estimates based on simulation studies [22]. Single electron injection is assumed at the left-most layer. The electron velocity is 10^7 cm/s and the hole velocity is 3×10^6 cm/s. A total of 34 incremental layers are used in the computations.

The frequency response has a 3-dB bandwidth of 8.5 GHz as shown in Fig. 4 (labeled *MQW*). The value of $J(f)$ at $f = 0$ is the area under the current response and corresponds to a gain of 15.5. Brennan [22] estimated the 3-dB bandwidth of this device as 9.2 GHz by using the approximate relation [19]

$$B = \frac{1}{2\pi m(\tau_e + \tau_h)} \tag{14}$$

where m is the number of stages, and τ_e and τ_h are the electron and hole transit times per stage, respectively. Clearly the assumption that the avalanche buildup time is negligible is not correct and even residual amount of hole ionization ($Q = 0.056$) is sufficient to reduce the bandwidth.

The impulse response is shown in Fig. 5. Time response is clearly nonexponential. However, the tail is exponential with a time constant of 19 ps. The initial response has multiple peaks corresponding to the arrival times of the original injected electrons and their first and second generations. The small lobes at the end of the frequency response correspond to these sharp peaks of the current. As compared with SAM-APD's of the same gain, MQW-APD's have much faster time responses and lower excess noise factor because of their short width and localized ionization layers. An expression for the excess noise factor F_e is readily available in the literature, and F_e for this device is 2.72 [22].

B. Conventional Multilayer APD

The second example is a three-layer InP/InGaAsP/InGaAs SAGM APD described by Osaka and Mikawa [14]. Two devices are considered with multiplication widths 2 μm (Fig. 2) and 1 μm (Fig. 3). They will be hereforth referred as SAM2 and SAM1, respectively. The photogeneration-rate profile is the same for both devices as shown in Fig. 2. The doping in the multiplication, grading, and absorption layers for both devices are 1.5×10^{16}, 1.0×10^{16}, and 1.0×10^{16} cm^{-3}, respectively. The spatial variations of electric field, depletion region width, carrier-ionization rates, and photogeneration rate are given by Osaka and Mikawa [14, eqs. 1-3, 8-9]. Ionization rate profiles are schematically shown in Figs. 2 and 3. For a gain of 15.5, the maximum field in SAM1 and SAM2 is 504.6 and 550.5 kV/cm, respectively. Electron and hole velocities are 10^7 and 5×10^6 cm/s, respectively. A total of 3000 incremental layers are used in the computations.

The frequency responses are the solid curves in Fig. 4 labeled (SAM1) and (SAM2). The low-frequency portion of these responses indicate that the impulse response dies off exponentially for large times. The multiple peaks at high-frequencies correspond to the onset of multiplication occurring during the first hole transit time. The dashed curves in Fig. 4 are obtained by Naqvi's formula for the

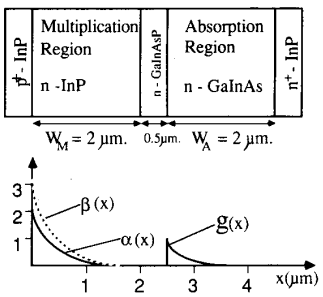

Fig. 2. The SAM2 device geometry and ionization-rate profiles for a three-layer InP/InGaAsP/InGaAs SAGM APD with a multiplication region width of 2 μm. Carrier ionizations occur essentially in the multiplication region. The photogeneration-rate profile $g(x)$ is shown schematically. The doping in the multiplication, grading, and absorption layers for both devices are 1.5×10^{16}, 1.0×10^{16}, and 1.0×10^{16} cm^{-3}, respectively. Photogenerated holes are injected from the left.

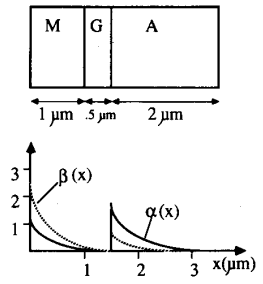

Fig. 3. SAM1. Same as SAM2 except that the multiplication region width is 1 μm. Carrier ionizations occur both in the multiplication and absorption regions. Photogeneration is not shown; it is same as in SAM2 but extends deeper into the absorption region.

current response due to an injected photoelectron [5, eq. 13 adjusted for hole injection]

$$J(\omega) = \frac{qM_n}{1 + j\omega M_n \tau_n}. \tag{15}$$

M_n is the mean gain given by (12) and τ_n is the "corrected intrinsic response time" for electrons

$$\tau_n = \frac{\kappa}{v_e + v_h} \int_0^W \exp\left[- \int_x^W (\alpha(x') - \beta(x'))\, dx' \right] dx \tag{16}$$

where κ is the "correction factor" to include the effect of carrier induced displacement current [30]. According to Naqvi [5] $\kappa \approx 0.5$ for $\beta/\alpha = 0.1$ and $v_e/v_h = 2$, and $\kappa \approx 1.5$ for $\beta = \alpha$ and $v_e = v_h$. The dashed curves in Fig. 4 are obtained for $\kappa = 1.0$ and 0.5 for SAM1 and SAM2, respectively. These curves show a similar low-frequency behavior. A precise low-frequency match can be obtained for SAM1 by adjusting the value of κ. Since Naqvi's theory neglects the divergence of the total current density in solving the transport equations, it does not predict the high-frequency response and is less accurate for high-speed devices. Clearly, Naqvi's formula does not account for the multiple peaks at high frequencies. The

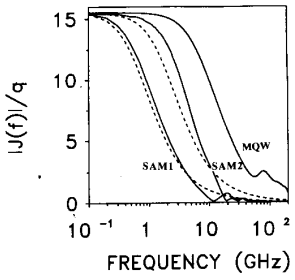

Fig. 4. Mean frequency responses of the three devices considered. The 3-dB bandwidth for MQW, SAM2, and SAM1 are 8.5, 3, and 0.8 GHz, respectively. The low-frequency behavior corresponds to the exponential tails of the corresponding time responses. The lobes at high frequencies corresponds to the peak of the time response. The dashed curves are obtained by Naqvi's theory [5], and they agree well for the low frequencies but differ at higher frequencies.

discrepancy with Naqvi's simplified theory is greater for SAM2 even for $\kappa = 0.5$ because it is a high-speed device, i.e., the half-power response time is comparable to the carrier-transit times.

The bandwidths for SAM1 and SAM2 are 0.8 and 3 GHz, respectively. Thus the multiplication in the absorption layer reduces the bandwidth considerably. Cambell *et al.* [9] report 3-dB bandwidths between 1.4 and 3.8 GHz at a gain of 10 for SAGM APD's with similar geometries to the ones considered here.

The time responses (Figs. 5 and 6) have sharp peaks corresponding to the hole transit time but, unlike the MQW APD, they decay smoothly. This is because carrier multiplication is equally likely to occur at any position in these devices. The tails are exponential with decay times of 200 ps for SAM1 and 53 ps for SAM2. Even though SAM2 has a faster response at the same gain, it suffers from low quantum efficiency. Quantum efficiencies for SAM1 and SAM2 are 0.75 and 0.23, respectively.

The design of such multilayer devices involves tradeoffs between the effects of transit times and the avalanche buildup time to attain high-gain, low-noise, and high-speed devices. The transit time is the time it takes for a carrier to transverse the device length. The response time is the time it takes for the carrier-multiplication process to end. Clearly the response time is greater than the transit time because of the avalanche buildup time. The speed of the device is governed by its response time. A short multiplication region enhances the speed of the device since it corresponds to shorter carrier transit times. This, however, results in an undesirable increase of the ionization rates in the absorption region due to the large electric field. This in turn increases the avalanche buildup time as well as increases the noise. In devices with longer multiplication region the electric field becomes sufficiently small so that no (or minimal) multiplication occurs in the absorption region. This, of course, comes at the expense of increased transit times and noise, and reduced speed. The results indicate that the former short-multiplication-region device (SAM1) is slower than the latter (SAM2),

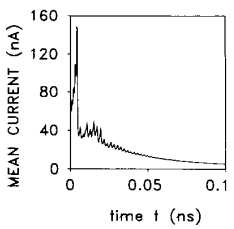

Fig. 5. The mean impulse response current as a function of time for the MQW APD. The first sharp peak corresponds to the first arrival time of the injected electron and the subsequent peaks are due to arrivals of secondary generations of electrons and holes.

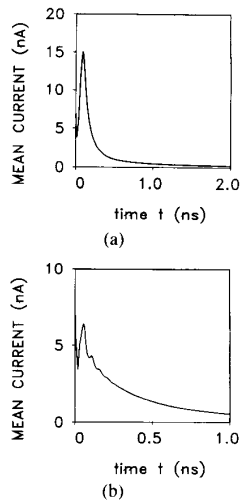

Fig. 6. The mean impulse response currents as a function of time for (a) SAM2 and (b) SAM1. The sharp peaks correspond to the arrival time of the injected holes. The time response of SAM1 is longer because it suffers from the multiplication in the absorption region, even though it has a shorter multiplication region width. The SAM2, on the other hand, suffers from low quantum efficiency, and instability at high bias voltages.

confirming that the effect of avalanche buildup time on device speed outweighs the effect of longer transit time. The latter device suffers less noise since it does not have concurrent multiplication and carrier injection which carry more uncertainty than localized lumped injection.

IV. Conclusion

We have derived equations for the time and frequency responses of APD's with arbitrary structures, including position-dependent ionization rates. The analysis also admits concurrent spontaneous or photo-induced electron-hole generation with an arbitrary distribution. This theory is applicable to different devices with varying architectures. The results have been used to determine the responses of two important structures whose time responses have not been accurately determined before. The dark current can also be studied by using a uniform thermal generation rate within each layer of the device. The hole accumulation at the heterojunction interfaces can be characterized by incremental layers in which the hole velocity is small.

Our results indicate that Naqvi's theory [5] underestimates the 3-dB bandwidth of the mean frequency response of a high-speed APD by neglecting the transient part of the current response assuming high gains and low-frequency modulation. Our method provides a more accurate evaluation of the 3-dB bandwidth of high-speed SAGM and superlattice MQW APD's in which the device gain is contained within the transient part of the impulse response.

We confirm the arguments and findings of Osaka *et al.* [14] regarding the exact evaluation of multiplication occurring in the absorption region. We find that the frequency response cannot be improved indefinitely by shortening the multiplication region and that tunneling is not the ultimate limit for it. Rather, it is the multiplication within the absorption region which increases the avalanche buildup time and makes the device noisier. This happens because shorter multiplication regions at the electric field levels sufficient to extend the depletion region into the absorption layer are also large enough to permit multiplication. This often makes the device unstable because of the very large ionization rates. On the other hand, if multiplication in the absorption region and instability were to be avoided by lowering the applied voltage, then the quantum efficiency would become unacceptably small. Therefore, an optimum structure with sufficiently large gain and quantum efficiency should be found for which both noise is suppressed and bandwidth is improved [31].

References

[1] R. B. Emmons and G. Lucovsky, "The frequency response of avalanching photodiodes," *IEEE Trans. Electron Devices*, vol. ED-13, pp. 297-305, 1966.

[2] R. B. Emmons, "Avalanche-photodiode frequency response," *J. Appl. Phys.*, vol. 38, pp. 3705-3713, 1967.

[3] C. A. Lee, R. L. Batdorf, W. Wiegmann, and G. Kaminsky, "Time dependence of avalanche processes in silicon," *J. Appl. Phys.*, vol. 38, pp. 2787-2797, 1966.

[4] J. F. Chang, "Frequency response of pin avalanching photodiodes," *IEEE Trans. Electron Devices*, vol. ED-14, pp. 139-145, 1967.

[5] I. M. Naqvi, "Effects of time dependence of multiplication process on avalanche noise," *Solid-State Electron.*, vol. 16, pp. 19-28, 1973.

[6] R. J. McIntyre, "Multiplication rates in uniform avalanche diodes," *IEEE Trans. Electron Devices*, vol. ED-13, pp. 164-168, 1966.

[7] A. A. R. Riad and R. E. Hayes, "Simulation studies in both the frequency and time domain of InGaAsP avalanche photodetectors," *IEEE Trans. Electron Devices*, vol. ED-27, pp. 1000-1003, 1980.

[8] S. Riad and A. Riad, "Time-domain simulation analysis of avalanche photodetectors," *IEEE Trans. Electron Devices.*, vol. ED-29, pp. 994-998, 1982.

[9] Y. K. Jhee, J. C. Campbell, J. F. Ferguson, A. G. Dentai, and W. S. Holden, "Avalanche buildup time of InP/InGaAsP/InGaAs with separate absorption, grading, and multiplication regions," *IEEE J. Quantum Electron.*, vol. QE-22, pp. 753-755, 1986.

[10] J. C. Campbell, W. S. Holden, G. J. Qua, and A. G. Dentai, "Frequency response of InP/InGaAsP/InGaAs avalanche photodiode with separate absorption 'grading' and multiplication region," *IEEE J. Quantum Electron.*, vol. QE-21, pp. 1743-1746, 1985.

[11] J. C. Campbell, A. G. Dentai, W. S. Holden, and B. L. Kasper, "High performance avalanche photodiode with separate absorption 'grading' and multiplication regions," *Electron. Lett.*, vol. 19, pp. 818-828, 1983.

[12] T. Shiba, E. Ishimura, K. Takahashi, H. Namizaki, and W. Susaki, "New approach to the frequency response analysis of an InGaAs av-

alanche photodiode," *J. Lightwave Technol.*, vol. 6, pp. 1502–1506, 1988.
[13] J. C. Campbell, S. Chandrasekhar, W. T. Tsang, G. J. Qua, and B. C. Johnson, "Multiplication noise of wide-bandwidth InP/InGaAsP/InGaAs avalanche photodiodes," *J. Lightwave Technol.*, vol. 7, pp. 473–487, 1989.
[14] F. Osaka and T. Mikawa, "Excess noise design of InP/GaInAsP/GaInAs avalanche photodiodes," *IEEE J. Quantum Electron.*, vol. QE-22, pp. 471–478, 1986.
[15] H. C. Hsieh and W. L. Sargeant, "Avalanche buildup time of an InP/InGaAsP/InGaAs APD at high gain," *IEEE J. Quantum Electron.*, vol. 25, pp. 2027–2035, 1989.
[16] K. Yasuda, T. Mikawa, Y. Kishi, and T. Kaneda, "Multiplication-dependent frequency responses of InP/InGaAs avalanche photodiodes," *Electron. Lett.*, vol. 20, pp. 373–374, 1984.
[17] K. Yasuda, T. Shirai, T. Kishi, S. Yamazaki, and T. Kaneda, "Heterojunction effect on spectral and frequency responses in InP/InGaAsP/InGaAs APD," *Japan J. Appl. Phys.*, vol. 22, pp. 291–204, 1982.
[18] D. T. Elkholm, J. M. Geary, J. N. Hollenhorst, V. D. Mattera, Jr., and R. Pawelek, "High bandwidth planar InP/InGaAs avalanche photodiodes," *IEEE Trans. Electron Devices*, vol. 35, p. 2433, 1988.
[19] K. Matsuo, M. C. Teich, and B. E. A. Saleh, "Noise properties and time response of the staircase avalanche photodiode," *IEEE Trans. Electron Devices*, vol. ED-32, pp. 2615–2623, 1985.
[20] M. C. Teich, K. Matsuo, and B. E. A. Saleh, "Time and frequency response of the conventional avalanche photodiode," *IEEE Trans. Electron Devices*, vol. ED-33, pp. 1511–1517, 1986.
[21] K. F. Brennan, Y. Wang, M. C. Teich, B. E. A. Saleh, and T. Khorsandi, "Theory of the temporal response of a simple multiquantum-well avalanche photodiode," *IEEE Trans. Electron Devices*, vol. 35, pp. 1456–1467, 1988.
[22] K. Brennan, "Comparison of multiquantum well, graded barrier, and doped quantum well GaInAs/AlInAs avalanche photodiodes: A theoretical approach," *IEEE J. Quantum Electron.*, vol. QE-23, pp. 1273–1282, 1987.
[23] R. S. Fyath and J. J. O'Reilly, "Frequency response characterization of superlattice avalanche photodiodes," *Proc. Inst. Elec. Eng.*, vol. 135, pt. J, pp. 413–422, 1988.
[24] P. Chakrabarti and B. B. Pal, "Optical characteristics of a superlattice avalanche photodiode," *Solid-State Electron.*, vol. 30, no. 7, pp. 675–679, 1987.
[25] —, "Theoretical characterization of a superlattice avalanche photodiode," *Appl. Phys. A—Solids Surfaces*, vol. 42, pp. 173–177, 1987.
[26] N. Z. Hakim, B. E. A. Saleh, and M. C. Teich, "Generalized excess noise factor for avalanche photodiodes of arbitrary structure," *IEEE Trans. Electron Devices*, vol. 37, pp. 599–610, 1990.
[27] J. N. Hollenhorst, "A theory of multiplication noise," *IEEE Trans. Electron Devices*, vol. 37, pp. 781–788, 1990.
[28] M. Y. Wu, "Solutions of certain classes of linear time varying systmes," *Int. J. Contr.*, vol. 31, pp. 11–20, 1980.
[29] —, "A successive decomposition method for the solution of linear time varying system," *Int. J. Contr.*, vol. 33, pp. 181–186, 1981.
[30] R. Kuvas and C. A. Lee, "Quasistatic approximation for semiconductor avalanches," *J. Appl. Phys.*, vol. 41, pp. 1743–1755, 1970.
[31] W. L. Sargeant, G. Kahraman, and B. E. A. Saleh, "Optimization of the InP/InGaAsP/InGaAs SAM avalanche photodiode," *J. Lightwave Technol.*, accepted for publication.

Gokalp Kahraman (S'90) was born in Izmir, Turkey. He received the B.S. degree from the University of Pennsylvania, Philadelphia, in 1986 and the M.S. degree from the University of Wisconsin, Madison, in 1988, both in electrical engineering.

He is currently working towards the Ph.D. degree at the University of Wisconsin—Madison, Department of Electrical and Computer Engineering. His research interests include physics of electronic and optoelectronic devices, optical amplifiers, optical communications, and quantum optics.

Bahaa E. A. Saleh (M'73-SM'86-F'91) received the B.S. degree from the Cairo University, Cairo, Egypt, in 1966 and the Ph.D. degree from the Johns Hopkins University, Baltimore, MD, in 1971, both in electrical engineering.

From 1971 to 1974 he was an Assistant Professor at the University of Santa Catarina, Brazil. Thereafter, he joined the Max Planck Institute in Gottingen, Germany, where he was involved in research in laser light scattering and photon correlation spectroscopy. He is presently Professor and Chairman of the Department of Electrical and Computer Engineering at the University of Wisconsin, Madison, where he has been since 1977. He held visiting appointments at the University of California, Berkeley, in 1977, and the Columbia Radiation Laboratory of Columbia University, New York, in 1983. He is currently involved in research in image processing, optical information processing, statistical optics, optical communication, and vision. He is the author of *Photoelectron Statistics* (Springer, 1978), and the coauthor of *Fundamentals of Photonics* (Wiley, 1991). He is currently the Editor of the *Journal of the Optical Society of America A* and a member of the Editorial Board of *Quantum Optics*.

Dr. Saleh is a Fellow of the Optical Society of America and John Simon Guggenheim Foundation, and a member of Phi Beta Kappa and Sigma Xi.

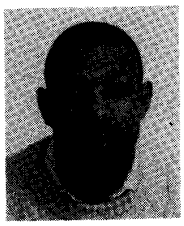

Winslow L. Sargeant (S'88) was born in Barbados, West Indies, on August 18, 1963. He received the B.S. degree from Northeastern University, Boston, MA, in 1986 and the M.S. degree from Iowa State University, Ames, IA, in 1988, both in electrical engineering.

Presently, he is working towards the Ph.D. degree, also in electrical engineering, at the University of Wisconsin, Madison. His research interests include device modeling and fabrication of avalanche photodiodes.

Mr. Sargeant is a member of NSBE, Eta Kappa Nu, and Sigma Xi.

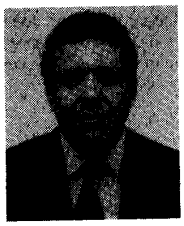

Malvin C. Teich (S'62-M'66-SM'72-F'89) was born in New York City. He received the S.B. degree in physics from the Massachusetts Institute of Technology, Cambridge, in 1961, the M.S. degree in electrical engineering from Stanford University, Stanford, CA, in 1962, and the Ph.D. degree in quantum electronics from Cornell University, Ithaca, NY, in 1966.

In 1966, he joined the MIT Lincoln Laboratory, Lexington, MA, where he was engaged in work on coherent infrared detection. In 1967, he became a member of the faculty in the Department of Electrical Engineering, Columbia University, NY, where he is now teaching and pursuing his research interests in the areas of quantum optics, optical and infrared detection, and sensory perception. He served as Chairman of the Department from 1978 to 1980. He is also a member of the faculty in the Department of Applied Physics, and a member of the Columbia Radiation Laboratory, the Center for Telecommunications Research, and the Fowler Memorial Laboratory at the Columbia College of Physicians and Surgeons. He has authored or coauthored some 150 technical publications and holds one patent. He is the coauthor, with B. Saleh, of *Fundamentals of Photonics* (Wiley, 1991).

Dr. Teich was the recipient of the IEEE Browder J. Thompson Memorial Price Award for his paper "Infrared Heterodyne Detection" in 1969, and in 1981 he received the Citation Classic Award of the Institute for Scientific Information for his work. He was awarded a Guggenheim Fellowship in 1973. He is a Fellow of the American Physical Society, the Optical Society of America, and the American Association for the Advancement of Science. He is a member of Sigma Xi, Tau Beta Pi, the Acoustical Society of America, the Association for Research in Otolaryngology, and the New York Academy of Sciences. He served as a member of the Editorial Advisory Panel for the journal *Optical Letters* from 1977 to 1979. He is currently Deputy Editor of the journal *Quantum Optics* and a Member of the Editorial Board of the *Journal of Visual Communication and Image Technology*.